

Temporal and Spatial Reservoir Ensembling Techniques for Liquid State Machines

Anmol Biswas
EE Dept. IIT Bombay
Mumbai, India
194076019@iitb.ac.in

Sharvari Ashok Medhe
EE Dept. IIT Bombay
Mumbai, India
20d070073@iitb.ac.in

Raghav Singhal
EE Dept. IIT Bombay
Mumbai, India
19d070049@iitb.ac.in

Udayan Ganguly
EE Dept. IIT Bombay
Mumbai, India
udayan@ee.iitb.ac.in

1

Abstract—Reservoir computing (RC), which is an umbrella term for a class of computational methods such as Echo State Networks (ESN) and Liquid State Machines (LSM) can be thought of as describing a generic method to perform pattern recognition and temporal analysis with any system having non-linear dynamics. This is enabled by the fact that Reservoir Computing is a shallow network model with only Input, Reservoir, and Readout layers and the input and reservoir weights need not be learned (only the readout layer is trained). LSM is a special case of Reservoir computing inspired by the organization of neurons in the brain and generally refers to spike-based Reservoir computing approaches. LSMs have been successfully used to showcase decent performance on some neuromorphic vision and speech datasets but a common problem associated with LSMs is that since the model is more-or-less fixed, the main way to improve the performance is by scaling up the Reservoir size, but that only gives diminishing rewards despite a tremendous increase in model size and computation. In this paper, we propose two approaches for effectively ensembling LSM models - Multi-Length Scale Reservoir Ensemble (MuLRE) and Temporal Excitation Partitioned Reservoir Ensemble (TEPRE) and benchmark them on Neuromorphic-MNIST (N-MNIST), Spiking Heidelberg Digits (SHD), and DVSGesture datasets, which are standard neuromorphic benchmarks. We achieve 98.1% test accuracy on N-MNIST with a 3600-neuron LSM model which is higher than any prior LSM-based approach and 77.8% test accuracy on the SHD dataset which is on par with a standard Recurrent Spiking Neural Network trained by Backprop Through Time (BPTT). We also propose receptive field-based input weights to the Reservoir to work alongside the Multi-Length Scale Reservoir ensemble model for vision tasks. Thus, we introduce effective means of scaling up the performance of LSM models and evaluate them against relevant neuromorphic benchmarks

Index Terms—liquid state machines, reservoir computing, ensemble models

I. INTRODUCTION

Reservoir Computing [1] is a general class of shallow network models that consist of Input, Reservoir, and output/classifier. In these models, only the output classifier weights are learned, the Input-Reservoir connections and the recurrent Reservoir connections are not learned, and the computational/representational power is derived from the complex dynamics of the Reservoir itself. It is this simplicity of

the Reservoir Computing model that allows it to convert potentially any system with complex dynamic behavior into a powerful computing unit. Liquid State Machines (LSM) [2] is a special case of Reservoir computing, where the Reservoir is composed of a population of spiking neurons with random and recurrent connections. Thus it is also a Spiking Neural Network (SNN) [3] and can be evaluated on neuromorphic benchmarks. In the absence of training (by design) in the Input and Reservoir layers, there is no universally accepted method to optimize the LSM setup. For example, NALSM [4] and P-Critical [5] propose modulated Spike time-Dependent Plasticity (STDP) to optimize the Input and Reservoir connections, [6] proposes a state-space model for fast evaluation of any given Reservoir connections matrix, MAdapter [7] proposes a kind of transfer learning for Input layer hyperparameters that have been optimized on any given dataset and SpiLinC [8] proposes an ensemble LSM model. MAdapter [7] also shows significant performance improvement by a process called time-partitioning but does not comment on the physical realizability of time-partitioning. In this paper, we adapt time-partitioning as a form of temporal ensemble model, called Temporal Excitation Partitioned Reservoir Ensemble (TEPRE) where each Reservoir in the ensemble only "sees" the input for a fixed fraction of the total presentation time of the sample. We also propose a Multi-Length Scale Reservoir Ensemble (MuLRE) model where each Reservoir in the ensemble has different underlying probability distributions for connecting neurons in the Reservoir, thus creating greater diversity in the representations generated by the ensemble model. Finally, we also propose a receptive-field-based input weight matrix for the LSM to preserve the spatial orderedness of vision input in the Reservoir as well. We evaluate all of our methods on standard neuromorphic benchmark datasets, i.e. NMNIST [9], SHD [10], and DVSGesture [11]. Code available at <https://github.com/SNNalgo/snntorch-LSM>

II. PROPOSED METHOD

A. Reservoir Neuron Model

The Reservoir neurons are Leaky-Integrate and Fire neurons described as follows [12]:

$$dv_i/dt = -v_i(t)/\tau_v + u_i(t) - \theta\sigma_i(t) \quad (1)$$

¹This work was presented at the International Conference on Neuromorphic Systems (ICONS) 2024, and has been accepted for inclusion in the conference proceedings

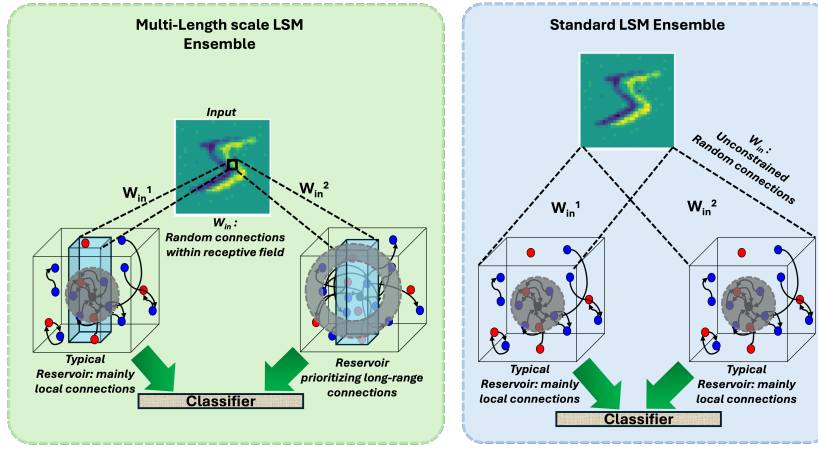


Fig. 1. Multi-Length Scale Reservoir Ensemble (MuLRE) compared against a standard LSM ensemble setup. MuLRE must use Receptive Field-based Input connections

$$u_i(t) = \sum_{j \neq i} w_{j,i} (\sigma_j * \alpha_u)(t) \quad (2)$$

$$\sigma_i(t) = \sum_t \delta(t - t_i^k) \quad (3)$$

Where $v_i(t)$ is the membrane potential of the i^{th} Reservoir neuron, $u_i(t)$ is the corresponding synaptic current, τ_v is the decay time constant of the membrane potential, $\sigma_i(t)$ is the spike-train of the i^{th} Reservoir neuron and θ is the spiking threshold

In eq. 2, $w_{j,i}$ is the weight connecting neuron j to neuron i where neuron i is always a Reservoir neuron, but neuron j can be either a different Reservoir neuron or an input neuron, and $\alpha_u(t) = (1/\tau_u)(e^{-t/\tau_u})H(t)$ is the synapse current kernel, where $H(t)$ is the *Heaviside* function and τ_u is the time constant of the synaptic current

For all of our simulations, we have set $\theta = 20$ and used $\Delta t = 1$ as the time-step

B. Input-Reservoir

1) *Standard Input*: For **Standard Input**, the Input is simply converted to a flat vector, and then an equal number of positive and negative connections are made from each input neuron to the Reservoir. The number of connections to be made is decided by the hyperparameter: **input connection density**, as described in [7] and [4]. In this paper, we use the MAdapter [7] method to set the Input layer hyperparameters **input weight** and **input connection density**

2) *Receptive Field-based Input*: For **Receptive Field-based Input**, the process of making connections from any Input neuron to the Reservoir does not change compared to **Standard Input**, but the pool of Reservoir neurons that an Input neuron can connect to changes. Instead of potentially being able to connect to any neuron in the Reservoir, now the input neuron can connect only to neurons within a narrow square window around the (x, y) co-ordinates in the Reservoir (the Reservoir is to be considered as a 3-D grid of neurons) that correspond

to the (x, y) co-ordinates of the input neuron in question. The window size is a hyperparameter and is set to 5 or 6 for our experiments. This restriction allows the spatial order of the visual input to be preserved even inside the Reservoir. This method of connecting Input to the Reservoir is visualized in Fig. 1

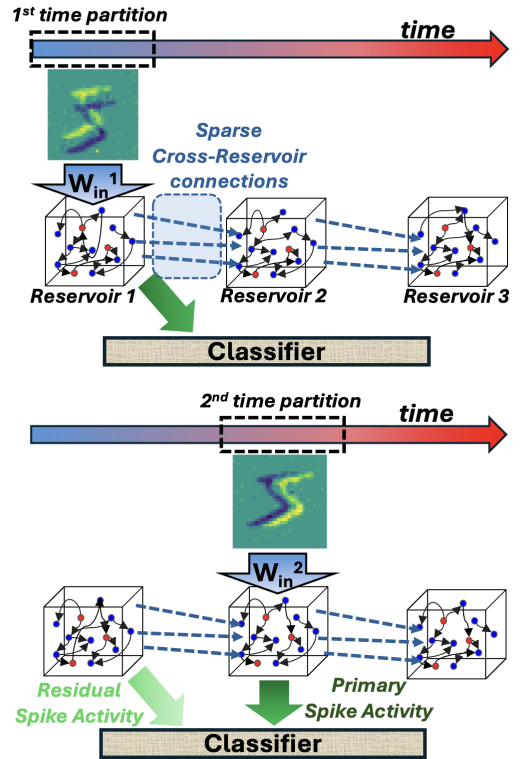


Fig. 2. Temporal Excitation Partitioned Reservoir Ensemble (TEPRE)

C. Reservoir Connections

The Reservoir is conceptualized as a 3-dimensional grid of spiking neurons, with dimensions N_x , N_y and N_z . Half

of the Reservoir neurons are excitatory and the other half are inhibitory. Generally, for a local probabilistic model of connectivity [13], connections between neuron i and neuron j within the Reservoir as made with the probability distribution:

$$Prob(i, j) = Cexp(-(D(i, j)/\lambda)^2) \quad (4)$$

Where $D(i, j)$ is the Euclidean distance between the two neurons. By default, this biases the Reservoir to prefer making short-distance connections between neurons. For the Multi-Length Scale Reservoir Ensemble model, we use a slight variation of this distribution function by introducing a distance term d as follows:

$$Prob(i, j) = Cexp(-((D(i, j) - d)/\lambda)^2) \quad (5)$$

This distribution biases connections for which the neurons are approximately d distance apart within the Reservoir. The weight value in the Reservoir, i.e. w_{lsm} from excitatory neurons and $-w_{lsm}$ from inhibitory neurons is set to 1 and the values of C to be used depend on the types of neurons i and j as described in [4]. For *excitatory-excitatory* connections, $C = 0.2$, for *excitatory-inhibitory* connections, $C = 0.1$, for *inhibitory-excitatory* connections, $C = 0.05$, and for *inhibitory-inhibitory* connections, $C = 0.3$

D. Ensemble Models

1) *Multi-Length Scale Reservoir Ensemble*: For the **Multi-Length Scale Reservoir Ensemble model** (MuLRE), we simply use different values of d depending on the number of reservoirs to be used for the ensemble. For 2-Reservoir ensemble, we use $d = \{0, 5\}$ and for 3-Reservoir ensemble, we use $d = \{0, 4, 6\}$. The MuLRE is always used in conjunction with Receptive Field-based Input. On the N-MNIST dataset, we observed best performance after preprocessing the incoming frames by a bank of 18 Gabor filters [14]. The ensemble setup is visualized in Fig. 1

2) *Temporal Excitation Partitioned Reservoir Ensemble*: For the **Temporal Excitation Partitioned Reservoir Ensemble** (TEPRE) we consider a number of smaller partition Reservoirs equal to the number of time partitions and schedule the input in such a way that it is received by one partition Reservoir within each time partition. The individual partition Reservoirs are interconnected with very sparse inhibitory connections that try to prevent successive partition Reservoirs from generating the same or highly correlated output. The operation of the TEPRE method is demonstrated in Fig. 2. For TEPRE experiments we use Standard Input only.

E. Classifier

In all of our experiments, we perform the final classification using a simple linear classifier (*linear_model* from *sklearn* library) [15]

III. EXPERIMENTS AND RESULTS

A. N-MNIST

We primarily test all of our proposed models on the N-MNIST dataset because it suits all the models being developed.

We use $\tau_u = \tau_v = 16$ for this dataset and test with different settings of number of partitions and ensemble configurations. Fig. 3 compares the two proposed methods against a vanilla ensemble LSM model and simple LSM (not ensemble) with an equal number of neurons. We find that the MuLRE significantly improves upon the vanilla ensemble LSM model, but is outperformed by the TEPRE model which achieves a test accuracy of 98.1% with a 3600-neuron reservoir and 3 partitions

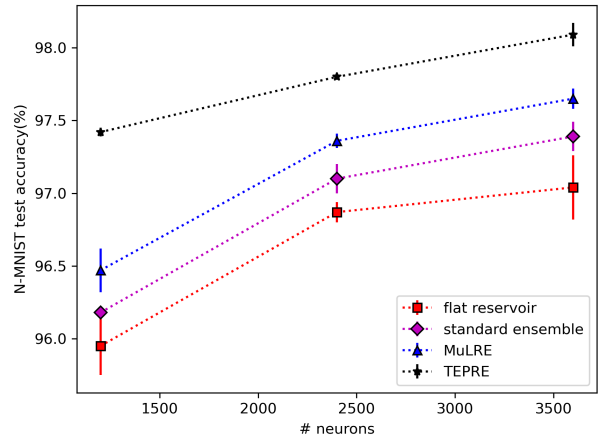


Fig. 3. Comparison of the different ensemble methods

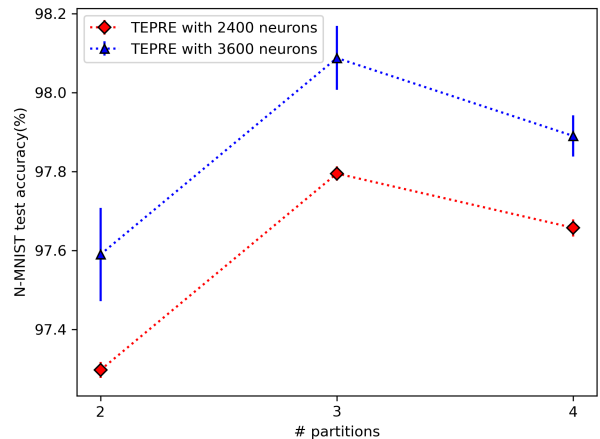


Fig. 4. Performance vs number of partitions

Fig. 4 compares the effect of increasing the number of partitions on the test accuracy and we find that 3 partitions is the optimal setting. This is expected considering that the N-MNIST dataset programs 3 temporally separate motions on the digit images. This indicates in the direction that the optimal number of partitions is likely to be decided by the underlying features of the data

B. SHD

The Spiking Heidelberg Digits [10] is a speech benchmark for Spiking Neural Networks. As the data consists of 1-D vector inputs at every time step, it is unsuitable for the MuLRE model. The dataset is read with `time_window=1000` in Tonic [16] and we tested it with the TEPRE model and achieved a maximum test accuracy of 77.8% using $(\tau_v, \tau_u) = (40, 20)$, $N_x = N_y = 10, N_z = 30$ and 6 partitions. This is comparable to the performance of a Recurrent Spiking Neural Network (RSNN) trained by BPTT [10].

C. DVSGesture

DVSGesture [11] dataset is a vision dataset where the task is to identify 11 gestures from their DVS camera recordings. Each input frame read with `time_window=20000` in Tonic [16] is 128x128x2 pixels, which we scale down to 64x64x2 before sending it to a $20 \times 20 \times 10$ ($N_x \times N_y \times N_z$) Reservoir using Receptive field-based input connections. Unfortunately, the DVSGesture dataset only contains 1000 training examples and it suffers from overfitting if any of the approaches discussed in this paper are applied. Under these restrictions, the maximum test accuracy achieved is 85.2% using $(\tau_v, \tau_u) = (5, 10)$, $N_x = N_y = 20, N_z = 10$ and 1 partition.

D. Comparison

TABLE I

Model	Learning	Accuracy	training params
Dataset: N-MNIST			
NALSM8000 [4]	astro-STDP + last layer Gradient descent	97.51%	80K
SLAYER [17]	Backpropagation	98.89%	1.41M
This work , 3600-neuron TEPRE, partition=3	last layer Gradient descent	98.1%	36K
This work , 3600-neuron Multi- Length Scale Reservoir Ensemble	last layer Gradient descent	97.65%	36k
Dataset: SHD			
This work , 3000-neuron TEPRE, partition=6	last layer Gradient descent	77.8%	30K
RSNN [10]	BPTT	79.9%	1.78M
Dataset: DVSGesture			
This work , 4000-neuron lsm with Standard input	last layer Gradient descent	82.8%	40K
This work , 4000-neuron lsm with Receptive Field-based input	last layer Gradient descent	85.2%	40K
Spiking CNN with 5 Conv layers and 2 Fully connected layers	Surrogate Gradient [18]	95.34%	5.38M

IV. CONCLUSION

In this paper, we propose two LSM ensemble models and one new LSM input approach that greatly improve the

performance and scaling of the LSM approach to temporal classification, both generally, and specifically for vision inputs. With these LSM ensemble models, LSM-based methods are approaching the standard learning-based baselines for N-MNIST and SHD benchmarks. This furthers the generalization of LSM and RC-based approaches. Future works could be finding suitable data augmentation techniques to improve the performance in the DVSGesture dataset for which the ensemble models overfit or implementing more complex neuron and synapse models, (including STDP) in the Reservoir to enhance its information representation properties

REFERENCES

- [1] M. Cucchi, S. Abreu, G. Ciccone, D. Brunner, and H. Kleemann, "Hands-on reservoir computing: a tutorial for practical implementation," *Neuromorphic Computing and Engineering*, vol. 2, no. 3, p. 032002, 2022.
- [2] W. Maass and H. Markram, "On the computational power of circuits of spiking neurons," *Journal of computer and system sciences*, vol. 69, no. 4, pp. 593–616, 2004.
- [3] W. Maass, "Networks of spiking neurons: the third generation of neural network models," *Neural networks*, vol. 10, no. 9, pp. 1659–1671, 1997.
- [4] V. Ivanov and K. Michmizos, "Increasing liquid state machine performance with edge-of-chaos dynamics organized by astrocyte-modulated plasticity," *Advances in neural information processing systems*, vol. 34, pp. 25703–25719, 2021.
- [5] I. Balafrej, F. Alibart, and J. Rouat, "P-critical: a reservoir autoregulation plasticity rule for neuromorphic hardware," *Neuromorphic Computing and Engineering*, vol. 2, no. 2, p. 024007, 2022.
- [6] A. Gorad, V. Saraswat, and U. Ganguly, "Predicting performance using approximate state space model for liquid state machines," in *2019 International Joint Conference on Neural Networks (IJCNN)*, pp. 1–8, IEEE, 2019.
- [7] A. Biswas, N. S. Nambiar, K. Kejriwal, and U. Ganguly, "Madapter: A multimodal adapter for liquid state machines configures the input layer for the same reservoir to enable vision and speech classification," in *2023 International Joint Conference on Neural Networks (IJCNN)*, pp. 1–6, IEEE, 2023.
- [8] G. Srinivasan, P. Panda, and K. Roy, "Spilinc: Spiking liquid-ensemble computing for unsupervised speech and image recognition," *Frontiers in neuroscience*, vol. 12, p. 524, 2018.
- [9] G. Orchard, G. Cohen, A. Jayawant, and N. Thakor, "Converting static image datasets to spiking neuromorphic datasets using saccades," *Frontiers in Neuroscience*, vol. 9, 2015.
- [10] B. Cramer, Y. Stradmann, J. Schemmel, and F. Zenke, "The heidelberg spiking data sets for the systematic evaluation of spiking neural networks," *IEEE Transactions on Neural Networks and Learning Systems*, 2020.
- [11] A. Amir, B. Taba, D. Berg, T. Melano, J. McKinstry, C. Di Nolfo, T. Nayak, A. Andreopoulos, G. Garreau, M. Mendoza, *et al.*, "A low power, fully event-based gesture recognition system," in *Proceedings of the IEEE Conference on Computer Vision and Pattern Recognition*, pp. 7243–7252, 2017.
- [12] M. Davies, N. Srinivasa, T.-H. Lin, G. Chinya, Y. Cao, S. H. Choday, G. Dimou, P. Joshi, N. Imam, S. Jain, *et al.*, "Loihi: A neuromorphic manycore processor with on-chip learning," *Ieee Micro*, vol. 38, no. 1, pp. 82–99, 2018.
- [13] W. Maass, T. Natschläger, and H. Markram, "Real-time computing without stable states: A new framework for neural computation based on perturbations," *Neural computation*, vol. 14, no. 11, pp. 2531–2560, 2002.
- [14] I. Fogel and D. Sagi, "Gabor filters as texture discriminator," *Biological cybernetics*, vol. 61, no. 2, pp. 103–113, 1989.
- [15] F. Pedregosa, G. Varoquaux, A. Gramfort, V. Michel, B. Thirion, O. Grisel, M. Blondel, P. Prettenhofer, R. Weiss, V. Dubourg, J. Vanderplas, A. Passos, D. Cournapeau, M. Brucher, M. Perrot, and E. Duchesnay, "Scikit-learn: Machine learning in Python," *Journal of Machine Learning Research*, vol. 12, pp. 2825–2830, 2011.

- [16] G. Lenz, K. Chaney, S. B. Shrestha, O. Oubari, S. Picaud, and G. Zarrella, "Tonic: event-based datasets and transformations.," July 2021. Documentation available under <https://tonic.readthedocs.io>.
- [17] S. B. Shrestha and G. Orchard, "Slayer: Spike layer error reassignment in time," *Advances in neural information processing systems*, vol. 31, 2018.
- [18] J. K. Eshraghian, M. Ward, E. Neftci, X. Wang, G. Lenz, G. Dwivedi, M. Bennamoun, D. S. Jeong, and W. D. Lu, "Training spiking neural networks using lessons from deep learning," *Proceedings of the IEEE*, vol. 111, no. 9, pp. 1016–1054, 2023.